NEUROPROSTHETICS

Neurorobotic fusion of prosthetic touch, kinesthesia, and movement in bionic upper limbs promotes intrinsic brain behaviors

Paul D. Marasco[1,2*†], Jacqueline S. Hebert[3,4†], Jonathon W. Sensinger[5†], Dylan T. Beckler[1‡], Zachary C. Thumser[1,6‡], Ahmed W. Shehata[3], Heather E. Williams[7], Kathleen R. Wilson[5]

Bionic prostheses have restorative potential. However, the complex interplay between intuitive motor control, proprioception, and touch that represents the hallmark of human upper limb function has not been revealed. Here, we show that the neurorobotic fusion of touch, grip kinesthesia, and intuitive motor control promotes levels of behavioral performance that are stratified toward able-bodied function and away from standard-of-care prosthetic users. This was achieved through targeted motor and sensory reinnervation, a closed-loop neural-machine interface, coupled to a noninvasive robotic architecture. Adding touch to motor control improves the ability to reach intended target grasp forces, find target durometers among distractors, and promote prosthetic ownership. Touch, kinesthesia, and motor control restore balanced decision strategies when identifying target durometers and intrinsic visuomotor behaviors that reduce the need to watch the prosthetic hand during object interactions, which frees the eyes to look ahead to the next planned action. The combination of these three modalities also enhances error correction performance. We applied our unified theoretical, functional, and clinical analyses, enabling us to define the relative contributions of the sensory and motor modalities operating simultaneously in this neural-machine interface. This multiperspective framework provides the necessary evidence to show that bionic prostheses attain more human-like function with effective sensory-motor restoration.

INTRODUCTION

Prosthetic interventions are showing increasing levels of sophistication. Controlling robotic devices has progressed beyond standard-of-care methods of moving single joints by pulling on the cables of body-powered gripper systems or reading binary myoelectric signals from remaining native muscles. Now, bionic approaches with surgical, implanted, and surface signal detection strategies access the intentional motor control signals directly from the brain and nerves (*1*–*3*). Avenues for providing prosthetic sensation have also been developed and are beginning to mature, allowing the activity of once insensate prosthetic limbs to be felt through appropriate feedback channels (*4*–*7*). Recently, combining advanced control and feedback with bone integration highlights the importance of building more integrated and clinically viable systems (*8*).

Touch and proprioception are the two primary components of somatosensation. Several approaches produce prosthetic touch, allowing users to feel contact and pressure (*9*–*20*). Proprioception, the sense of joint position and movement in space, has been more difficult to implement in a closed-loop system (*21*). Hand and finger position percepts from neural stimulation have been described from early work (*22*) to modern approaches for transradial amputation (*15*, *19*, *23*–*25*). Hand postures can be determined through combinations of electrically induced sensory percepts (*26*). Coupling tactile and proprioceptive percepts together along with a native muscular surface myoelectric controlled task demonstrated object size and compliance discrimination with a detached prosthetic hand (*25*). Electrically induced touch and proprioceptive feedback in a system that used myoelectric control from the residual native forearm muscles showed improvements in discriminating the presence or absence of an object in the hand (*14*) and object size and compliance (*24*). These improvements were achieved by mapping prosthetic hand aperture to either a percept of digit flexion or to a proportional touch percept. Discrimination of size and compliance have also been shown in a native residual forearm muscle myoelectric control interface coupled with electrically induced touch feedback and pure substitution of electrically induced paresthesias linking current amplitude to hand aperture (*19*). Although learning over time may enhance the use of these signals for closed-loop function (*25*, *27*), performance benefits from sensory substitution methods do not typically extend to meaningful unconstrained prosthetic use in the presence of vision (*4*, *8*).

A common constraint of advanced sensory-motor prosthetic systems is their restriction to distal amputation levels because of the necessity of using the intact proximal forearm muscles for native myoelectric control (either surface or implanted) (*5*). Function in these systems is likely improved with the residual musculature as part of the control interface (*23*, *24*, *28*). However, the proprioceptive information from the remaining muscles makes it difficult to parse out the relative contributions of neurally induced sensory feedback. A promising approach uses natural agonist/antagonist muscle pairings through surgical tendon connections to provide biaxial control

[1]Laboratory for Bionic Integration, Department of Biomedical Engineering, Lerner Research Institute, Cleveland Clinic, 9500 Euclid Avenue, ND20, Cleveland, OH 44195, USA. [2]Advanced Platform Technology Center, Louis Stokes Cleveland Department of Veterans Affairs Medical Center, 10701 East Boulevard 151 W/APT, Cleveland, OH 44106, USA. [3]Division of Physical Medicine and Rehabilitation, Department of Medicine, University of Alberta, Edmonton, Alberta T6G 2E1, Canada. [4]Glenrose Rehabilitation Hospital, Alberta Health Services, 10230-111 Avenue, Edmonton, Alberta T5G 0B7, Canada. [5]Institute of Biomedical Engineering, University of New Brunswick, 25 Dineen Drive, Fredericton, New Brunswick E3B 5A3, Canada. [6]Research Service, Louis Stokes Cleveland Department of Veterans Affairs Medical Center, 10701 East Boulevard, Research 151, Cleveland, OH 44106, USA. [7]Department of Biomedical Engineering, University of Alberta, Edmonton, Alberta T6G 2E1, Canada.
*Corresponding author. Email: marascp2@ccf.org
†Co–senior authors.
‡These authors contributed equally to this work.

and proprioception for prosthetic ankles (*29*, *30*). However, the complex multiaxial agonist/antagonist forearm and intrinsic hand muscle relationships controlling the fingers and wrist are likely less amenable to this type of interface. In the absence of the intact distal anatomy, kinesthetic perception of hand grip movements after targeted muscle reinnervation allowed participants with proximal amputation to attain able-bodied performance in a hand prepositioning task by coupling kinesthesia and motor control (*31*).

Although pioneering efforts have revealed individual facets of sensory-motor synthesis, the complex interplay between neurally derived motor control, proprioception, and touch that is the hallmark of upper limb function has not yet been revealed in bionic prostheses. Moreover, comparing the contributions of touch, proprioception, and motor control to overall function in the context of able-bodied performance has not been possible. Psychophysical tools are effective for probing sensory and perceptual responses to different stimuli. However, assessments often lack functional correlates, which confounds interpretation of potential benefits. Clinical motor-focused prosthetic performance evaluations rely on qualitative practitioner assessment, subjective reporting, or speed-based measures (*32*–*35*) that typically lack sensitivity. Also, they do not challenge to the level of able-bodied performance (ceiling effects), and they do not capture the effects of sensory integration. The advantages of bionic prosthetic systems are rendered invisible, which obscures the potential benefits of new technologies and treatments over standard of care (*9*, *24*, *36*).

To address these limitations, we constructed a suite of functional metrics to quantify the performance of sensory-motor bionic systems within the continuum spanning basic standard-of-care prostheses to the gold standard of able-bodied performance. The metrics focus on essential sensory-motor features of limb function such as visual attention, cognitive demand, fine motor dexterity, and ownership while also being clinically and real-world relevant. Each metric was validated in their foundational fields of psychophysics, mathematical theory, cognition/perception, visuomotor behavior, and psychometrics (*23*, *31*, *37*–*54*).

In this study, we reveal functional improvements from the simultaneous integration of touch, kinesthesia, and movement intent within bidirectional bionic upper limb prosthetic systems. In two participants with proximal arm amputation, the neurorobotic fusion of touch, kinesthesia, and intuitive motor control promoted performance levels that were stratified toward able-bodied functional behaviors and away from standard-of-care prosthetic users. Our theoretical and clinical evaluation strategy reveals a coherent picture of a complex natural system by quantifying the influence of sensory modalities on grasp modulation, visuomotor behavior, decision strategy, internal model function, and ownership. This evaluation framework revealed that integrating the bionic modalities of touch, kinesthesia, and motor control together led to more human-like system function.

RESULTS

Neural-machine interface participants

For two individuals with high-level upper limb amputation, we developed self-contained bionic prosthetic limbs controlled by signals of intentional hand, wrist, and elbow movements while simultaneously providing proprioceptive and touch feedback (Fig. 1). We used targeted reinnervation as the bidirectional sensory-motor neural-machine interface.

Targeted muscle reinnervation (TMR-motor) surgically reassigns neural control of the muscles remaining above the amputation. The purposely denervated biceps and triceps of participant TH (pTH) and pectoralis and latissimus dorsi of participant SD (pSD) were reinnervated with their amputated median, radial, and ulnar hand nerves to serve as biological amplifiers for their neural motor command signals. When the participants made intentional movements of their missing limbs, the neurally reassigned muscle contractions were read at the skin surface with electromyographic electrodes to command the prosthetic hand and arm motors simultaneously (*55*).

Targeted sensory reinnervation (TSR-touch) provided the neural-machine interface for touch. Remaining proximal skin was denervated to provide reinnervation targets for sensory nerves (median and ulnar) surgically redirected from the missing limb (*56*, *57*). Touching the neurally reassigned skin activates reinnervated sensory terminals to generate tactile percepts that are projected to the missing hand (*58*–*61*) and interpreted as being their own hand (*62*). Small neurorobotic touch tactors pressed into the appropriate touch percepts in the skin to generate sensation whenever the fingers of the prosthetic hand contacted objects (*9*), thus providing physiologically relevant sensation for pTH's thumb, index, and middle fingers and pSD's thumb, index, middle, ring, and little fingers and palm.

TMR also reassigns the proprioceptive sensory-neural structure of the target muscles to provide kinesthetic perception of active complex grip conformations that are projected to the missing hand (TSR_m-kinesthesia) (*31*). Hand-close grip percepts in the deep muscle were identified for pTH and pSD. A small neurorobotic kinesthetic tactor mounted to the prosthetic socket applied 90-Hz vibration to percept locations whenever the prosthetic hand physically closed. The participants felt their own hand moving from an open to a closed position at the speed of their prosthetic hand. TSR_m-kinesthesia turned off when the prosthetic hand stopped moving, either through TMR-motor control or when encountering noncompressible objects.

Neurally derived motor control, kinesthesia, and touch all operated simultaneously in a stand-alone prosthetic upper limb system. All control and feedback modalities ran independently with their own on-board computer processing systems. TMR-motor control and TSR-touch were powered by the on-board prosthetic limb battery, and TSR_m-kinesthesia was powered by a wearable battery. The system was iterated within the form factor and functional constraints of a commercial motorized myoelectric prosthetic limb (fig. S1).

Foraging for specific stiffness blocks among distractors

Grasping and manipulating objects require a balance of motor control and sensation. The Prosthesis Efficiency and Profitability (PEP) assessment uses optimal foraging theory mathematics to quantify how efficiently individuals use feedback to inform sensory discrimination decisions in relation to overall motor performance (*49*). Participants searched for, located, and sorted small rubber stiffness-specific blocks from distractor blocks (Fig. 2A) while wearing frosted glasses and noise-cancelling headphones. To provide context for comparison, cohorts of able-bodied participants and individuals with amputation using body-powered and two-site sequentially controlled native myoelectric prostheses were evaluated with the PEP test.

Assessing the time-focused block-sorting decision performance (Fig. 2, B and C) showed that with adding TSR-touch, both pTH and pSD's sorting accuracy improved above TMR-motor alone, but they took more time to complete the task (figs. S2 and S3A). This trade-off

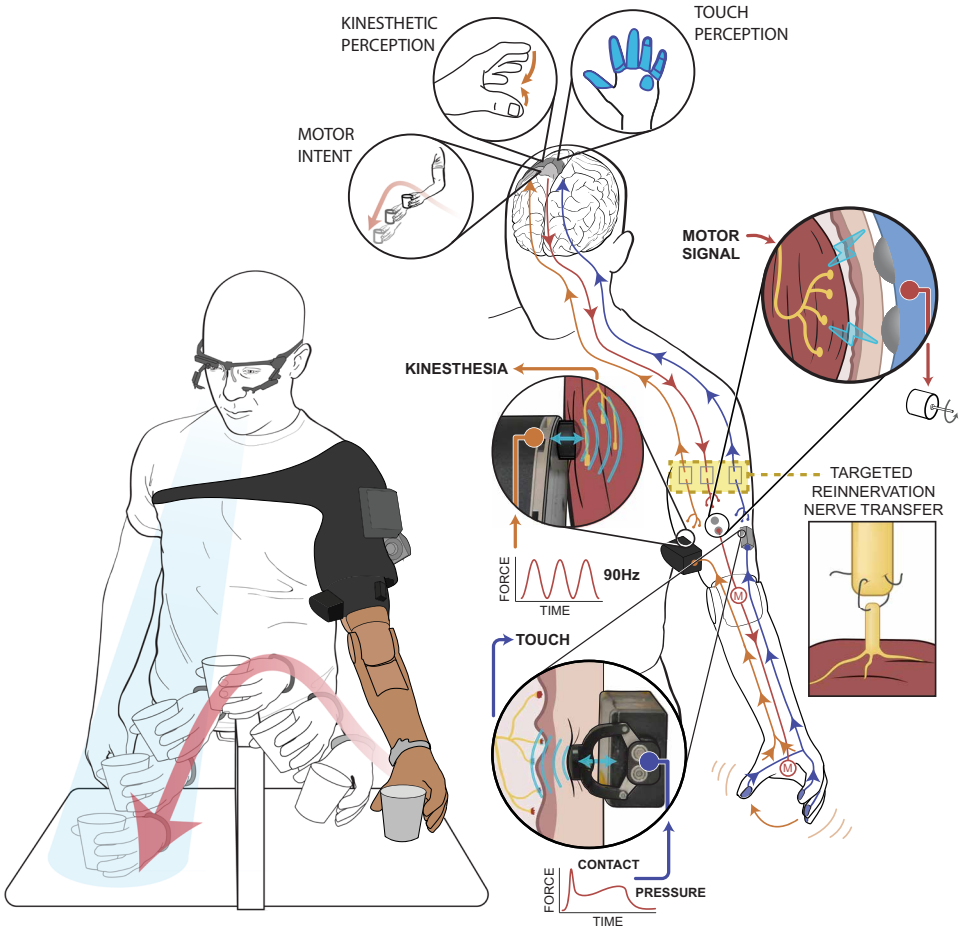

Fig. 1. The simultaneous integration of touch, kinesthesia, and movement intent within a neurorobotic human-integrated bidirectional bionic upper limb prosthetic system. The combination of targeted muscle reinnervation (TMR) and targeted sensory reinnervation (TSR) creates a bidirectional connection between the participants' nervous systems and their robotic prosthetic limbs. They think about moving their arm (TMR-motor intent), and the electrical signals from the neurally reassigned limb muscles are read by electromyographic surface electrodes and translated to the appropriate prosthetic movements. Prosthetic fingertip sensors recognize touch events and relay them to touch robots that translate the sensory events into displacements that activate neurally reassigned touch receptors in the target skin of the proximal limb (TSR-touch). A potentiometer reads prosthetic hand movement to activate a kinesthetic robot that sends 90-Hz vibration to the deep sensory receptors of the muscles reinnervated by TMR (TSR_m-kinesthesia) for activation of complex kinesthetic hand closure percepts.

resulted in flat values for target stiffness discrimination efficiency and overall system performance (Fig. 2, B and C). However, when both TSR-touch and TSR_m-kinesthesia were added, pTH and pSD's stiffness discrimination accuracy improved significantly above TMR-motor alone (pTH, 68 to 81%, $P = 0.017$; pSD, 42 to 83%, $P < 0.0001$; table S1), approaching the low end of able-bodied accuracy (fig. S2A). Their recognition speed and handling speed also increased, significantly so for pSD (recognition time of 7.75 to 4.01 s, $P < 0.0001$; handling time of 4.53 to 2.57 s, $P < 0.0001$; fig. S2 and table S1). Using TSR-touch and TSR_m-kinesthesia with TMR-motor control elevated the performance of pTH and pSD with proximal amputations to the level of highly functional body-powered and native myoelectric users with distal amputations (see text S1).

PEP reveals the search strategies used during discrimination tasks. There are two types of discrimination task errors: (i) mistakenly choosing the wrong stiffness block, which negatively affects the participant's score (false-positive rate: alpha; fig. S3B), and (ii) putting back a correct block (false-negative rate: beta; fig. S3C), which does not reduce the score directly but costs time. The ternary plot in Fig. 3 shows the mathematical relationships underlying discrimination strategy mistake patterns (fig. S4). The green dashed line depicts a balance between three elements: (i) completing the task quickly, (ii) taking the time to discriminate, and (iii) focusing on the most payoff for effort applied. Moving along each contour line shows changes in used strategy (pace maximizing or accuracy maximizing). Moving across contour lines shows changes in system performance (see text S1).

pTH and pSD's system performance improved with each sensory modality. With TMR-motor control only, pSD could not discern block stiffness and focused instead on quickly picking the first block that could be grasped reliably, similar to a body-powered participant (Fig. 3). pSD's position at the lower left apex of the ternary plot reveals her focus on speed (left of the teal dashed line) instead of accuracy with discrimination decisions slightly above a chance (the black dashed line). With the addition of TSR-touch, pSD could accurately discern block stiffness, thereby gaining system performance (moving across contour lines) and shifting her to a balanced discrimination strategy (green dashed line). TSR-touch with TSR_m-kinesthesia further elevated pSD's system performance and discrimination strategy balance (slightly favoring speed), thereby stratifying with able-bodied participants above pTH, the native myoelectric prosthesis users, and the body-powered users who resided at the extremes of the selection strategies. With TMR-motor control only, pTH already used a balanced discrimination strategy with system performance aligned with body-powered and native myoelectric users. TSR-touch improved pTH's system performance while maintaining a balanced discrimination strategy. With TSR-touch, TSR_m-kinesthesia, and TMR-motor intent together, pTH improved further, stratifying near pSD at the lower end of able-bodied system performance and discrimination strategy balance.

Visuomotor assessment during functional tasks

Visual allocation during coordinated object interaction is an integral component of sensory-motor performance. Standard-of-care prosthesis users have abnormally increased visual fixation on their prosthetic hands when reaching for and transporting objects (*45*). The Gaze and Movement Assessment (GaMA) protocol (*44*) quantified visual fixations (*42*) and movements (*43*) of participants as they

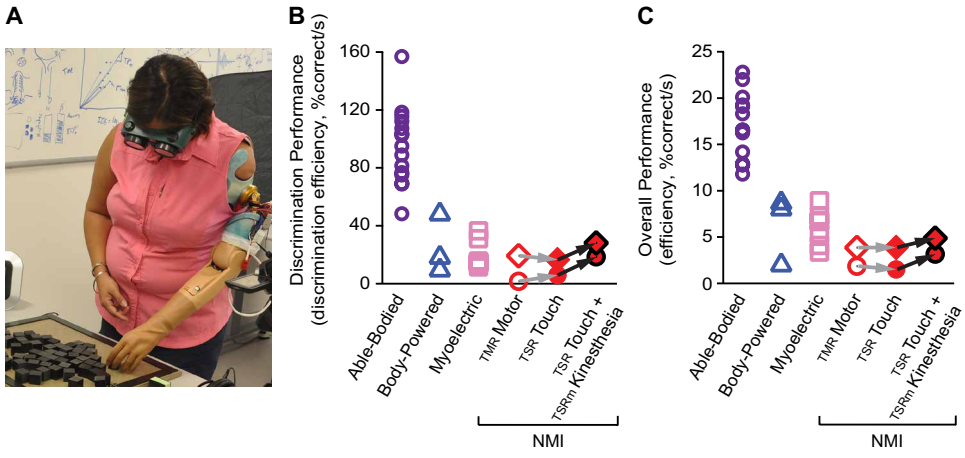

Fig. 2. Neurorobotic kinesthesia, touch, and motor intent improve system efficiency. (**A**) Participant performing the PEP task. (**B**) Discrimination performance measures a user's individual sorting decisions. The *y* axis shows discrimination performance in profitability (% of correct blocks per second; i.e., the ability to identify correct blocks weighted against the time taken to identify each block). (**C**) Overall system efficiency is a measure of the overall efficiency of the prosthetic system. The *y* axes show each participant's efficiency score, measured in "% of correct blocks per second," i.e., the ability to identify correct blocks weighted against the time taken to complete the entire task trial. Red circle, pSD; red diamond, pTH; TSR_m, TSR of the muscle for kinesthesia; NMI, neural-machine interface.

picked up and transferred paper cups full of beads over a barrier (Fig. 4A, text S2, and table S2) (*41*).

When reaching for the cups, pTH and pSD fixated to the prosthetic hand significantly less when provided with TSR_m-kinesthesia and TSR-touch compared with TMR-motor only (pTH, 1.70% ± 4.45 versus 3.65% ± 5.95, $P = 0.028$; pSD, 13.59% ± 14.55 versus 22.78% ± 16.31, $P = 0.027$; Fig. 4B and tables S3 and S4). This result suggests that pTH and pSD had increased confidence in grip aperture preparation for cup grasping.

When transporting the cup to a new target location, there were significantly fewer fixations to the hand/cup when the participants had TSR-touch and TSR_m-kinesthesia compared with both TSR-touch only and to TMR-motor only (pTH, 12.92% ± 8.43 versus 18.35% ± 8.04, $P < 0.0005$ and versus 16.78% ± 8.11, $P = 0.10$; pSD, 49.10% ± 10.53 versus 57.48%, $P = 0.001$ and versus 58.26% ± 9.11, $P < 0.005$; Fig. 4C and tables S3 and S4). For pSD, fusion of TSR-touch and TSR_m-kinesthesia with TMR-motor intent resulted in reduced visual fixation to the hand during cup transport and a significant increase in gaze to the next placement target location (35.73% ± 7.33 versus 30.42% ± 8.67, $P = 0.028$; tables S3 and S4). The primary risk during transport was crushing the cup. TSR_m-kinesthesia likely reduced undesired hand closure, which allowed both participants to adopt more able-bodied visual allocation behaviors. Because of technical challenges, pTH operated with a locked elbow and a 1–degree of freedom (open/close) hand (see the "Study limitations and next steps" section and text S2). His performance was within the interquartile range of able-bodied for all conditions because he was likely using his intact proximal shoulder for proprioception. However, even with a high level of baseline performance with TMR-motor, he improved with neurorobotic sensory-motor fusion, approaching the able-bodied median values for percent hand/cup fixation for both reach and transport when both TSR-touch and TSR_m-kinesthesia were provided (see dashed lines in Fig. 4, B and C).

Because of pTH's technical challenges, only pSD could perform the complex task of turning to the side to grasp a pasta box outside of the forward visual field and transporting it to shelves of varying height and location. In this task, pSD showed near normalization of visual fixations to her hand when provided with both TSR-touch and TSR_m-kinesthesia (Fig. 4D). Releasing the gaze from the prosthetic hand is critical for functionally attending to the next planned action. With TSR-touch and TSR_m-kinesthesia, pSD showed significant improvements (approaching able-bodied performance) in percent fixations to the next target location compared with TMR-motor only (64.03% ± 8.47 versus 51.81% ± 11.57, $P = 0.043$; Fig. 4E and tables S5 and S6).

Bidirectionally integrated prosthetic limb ownership

Bionic limbs that not only sense the environment but also transmit those sensations to the user start to blur the divisions between human and machine (*63*). Multisensory integration is the substrate for incorporating a bionic prosthesis into the user's self-image and providing them with the sense that the limb is part of their body (*62*, *64*–*67*). Movement intent and movement sensation combine to provide agency over a prosthesis, the sense that the movements of the limb are their own (*31*). We used the Dynamic Prosthesis Incorporation (PIC) assessment to evaluate neurorobotic prosthesis incorporation into the user's self-image, a cognitive feature that may influence prosthesis acceptance (*68*). We used the crossmodal congruency effect (text S3) to quantify ownership by measuring grasping task reaction time to visually congruent and incongruent distracter lights on a neurorobotic hand (Fig. 5A).

pSD showed high ownership with TSR-touch alone (Fig. 5B), within the lower range of intact physiology (*52*). However, her PIC score was slightly reduced with the addition of TSR_m-kinesthesia. It is difficult to draw firm conclusions from pSD because a technical code issue caused inconsistent kinesthetic tactor activity during hand closing, which may have negatively affected the already strong ownership response to touch feedback. Scores for pTH were on par with physical skin deformation in able-bodied participants (*52*). TSR_m-kinesthesia together with TSR-touch increased the sense of ownership, providing evidence that TSR-touch and TSR_m-kinesthesia with TMR-motor intent helped pTH to feel his prosthetic hand as his own hand over touch alone.

Intended grasp force speed/precision relationships

Prosthetic touch must be integrated effectively in the sensory-motor control loop to improve function. We used the Grasping Relative Index of Performance (GRIP) test to examine the ability of individuals to use touch feedback to achieve intended grip forces. GRIP uses Fitts' law to evaluate the trade-offs between speed (completing tasks quickly) and precision (reaching targets precisely) when applying grasping forces (*47*). We showed participants images of everyday objects (fig. S5A) (*23*). They then quickly squeezed a manipulandum (hidden from view) with the estimated force they thought would be required to pick the objects up (Fig. 6A, text S4, and fig. S5).

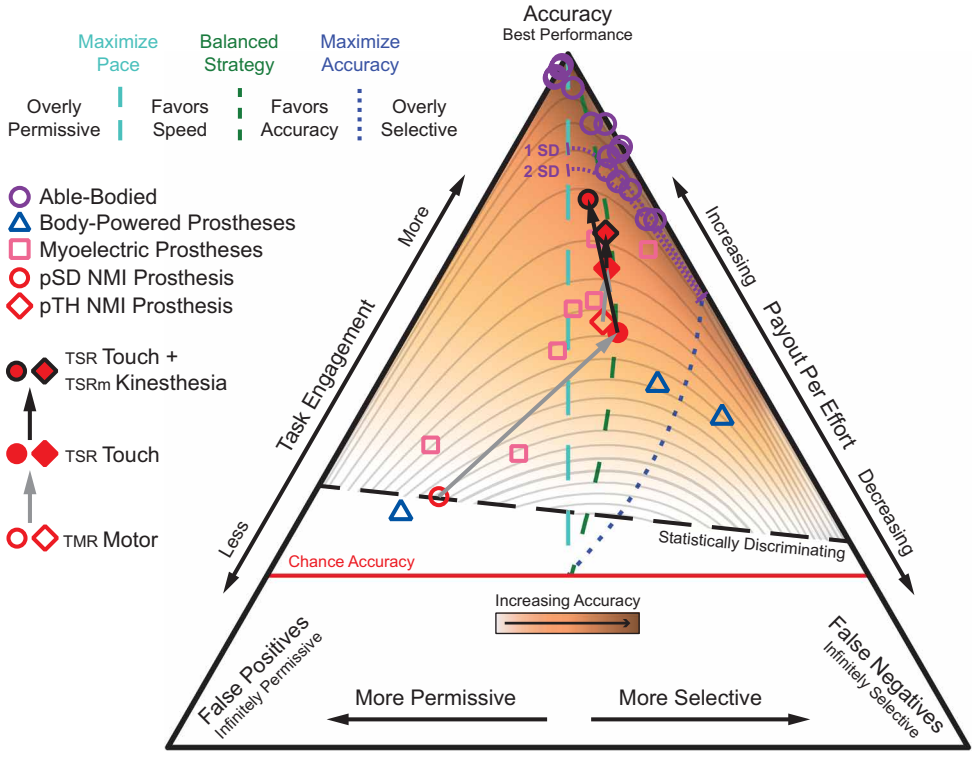

Fig. 3. Neurorobotic kinesthesia, touch, and motor intent stratify neural-machine interface participants with able-bodied performance. The PEP ternary plot describes a participant's strategic interplay between making false-positive errors [choosing the wrong block (bottom left vertex)], false-negative errors [discarding the correct block (bottom right vertex)], and final accuracy (top vertex). Each vertex represents 100% of the respective variable, with the opposite side representing 0%. The copper gradient shows final accuracy. The purple dotted contour bars show 1 and 2 SD from the average of the able-bodied false-positive and false-negative error product. The vertical cyan dashed line represents a strategy where participants maximize pace, i.e., maximizing accuracy while minimizing block encounters. Data points to the left of this line are too permissive and would benefit by increasing selectivity. The blue dotted line represents a strategy that maximizes accuracy. Data points to the right of this line are overly selective and would benefit by increasing permissiveness. Points between the cyan and blue lines represent strategic trade-offs between the two edge strategies. The green dashed line represents a balanced strategy where speed and accuracy trade-offs are optimized. The horizontal red line is chance accuracy. Performance above the black dashed line represents statistically significant performance better than expected chance. Changes in a participant's strategy results in moving along the gray contour lines, whereas changes in system performance results in moving across the contour lines.

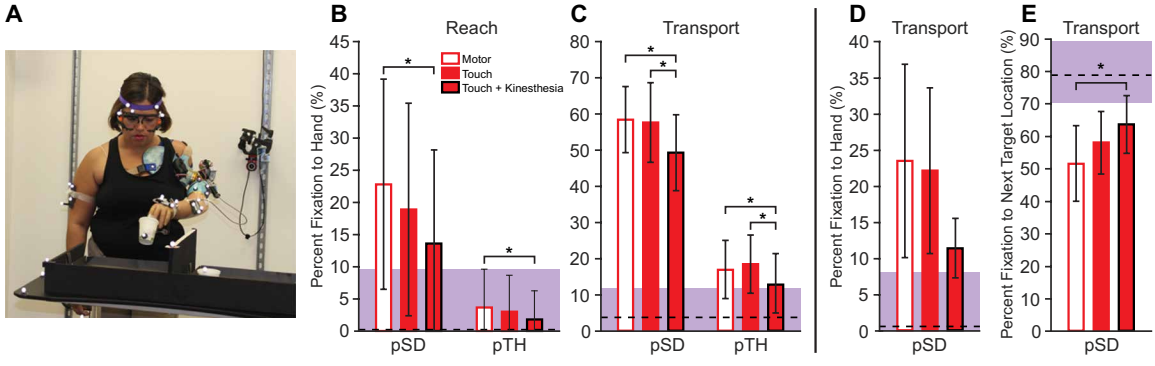

Fig. 4. Less visual fixation to the prosthetic hand is required with neurorobotic kinesthesia, touch, and motor intent. (**A**) Participant performing the cup transfer task for the GaMA. The dashed line and shading in (**B**) to (**E**) represent the normative median fixation and interquartile ranges for each measure. (B) Percent visual fixation to the prosthetic hand during averaged reach phases and (C) averaged transport phases for participants pSD and pTH. (D) Percent fixation to hand during averaged transport phases when pSD performed the pasta box transfer task and (E) percent fixation to the next target location during transport. All error bars represent ±1 SD.

Providing pSD and pTH with TSR-touch increased the number of objects successfully handled over TMR-motor only (orange to green color change in Fig. 6B). TSR-touch also improved their ability to reliably produce a force on the manipulandum; the transition from below to above the red dashed line denotes where applied forces were statistically indistinguishable from no force applied (Fig. 6B).

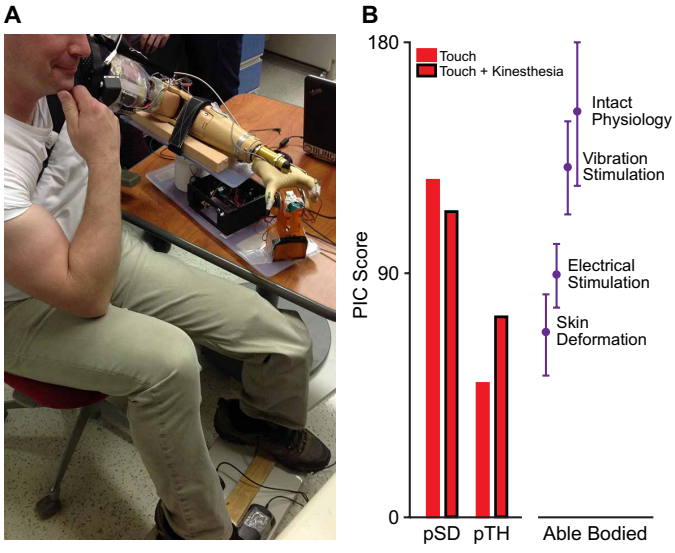

Fig. 5. Participants show high ownership scores with neurorobotic feedback. (**A**) A participant performing the Dynamic PIC assessment. (**B**) Dynamic PIC scores for participants pTH and pSD. Mean Dynamic PIC scores and SD at the 95% confidence interval (means ± 1.96 × SD) for intact physiology (*96*) and for skin deformation, electrical stimulation, and vibration stimulation with participants using a simulated prosthesis (*52*) are shown for reference.

TSR-touch improved the speed relative to how precisely pTH and pSD could achieve target forces (throughput in bits per second). Both participants showed a decreased variability (increased precision) around intended target forces [maximum index of difficulty (IDe) in bits]. Both improvements were indicated by the right and upward position of TSR-touch (filled circle) related to TMR-motor control only (filled square). For real-world context, we tested individuals with distal amputations using body-powered and native myoelectric prostheses and also present previously published benchmark values for able-bodied GRIP test performance (*47*).

Although GRIP was expressly designed to test touch, we examined TSR-touch and TSR_m-kinesthesia to explore interactions between these modalities. Because the GRIP manipulandum was uncompressible, when the prosthetic fingers made contact, they stopped moving, which turned TSR_m-kinesthesia off. We anticipated that without finger movement, TSR_m-kinesthesia would not likely improve performance. We found that TSR-touch coupled with TSR_m-kinesthesia decreased peak precision and reduced the number of objects successfully handled for both pTH and pSD. However, we found that TSR-touch and TSR_m-kinesthesia appeared to increase throughput for both participants in relationship to their baseline TMR-motor–only condition (Fig. 6B and fig. S5, D to H).

Adaptation rate in sensory-motor control

Performance limitations for bionic prostheses can be related to many domains. Feedback modality, somatotopic register (location), sensory naturalness, motor control system approach, training, and system noise may influence integration effectiveness. We used inductive Bayesian approaches, leveraging psychophysical models, as a tool to disentangle these relevant features. We measured trial-by-trial adaptation to participants' intrinsic error corrections while catching a falling bar with their prosthetic hand such that it stopped in alignment with a target (text S5 and fig. S6). Adaptation rate depends on the quality of control noise and sensory feedback. Adaptation rate increases with relevant sensory information, whereas low adaptation rate indicates mistrust in sensory feedback (*69*).

We tested pTH with visual feedback and TSR-touch and then with visual feedback and TSR-touch + TSR_m-kinesthesia. We found that TSR-touch together with TSR_m-kinesthesia increased adaptation rate for pTH from (1.51 ± 0.06) to (2.22 ± 0.20) (Fig. 7). Performance also improved in average error (−2.9 to >0.3 cm) and variance (16.4 to >11.02 cm^2), significantly so ($P = 0.004$). pTH appeared to rely on TSR_m-kinesthesia to improve performance, even in the presence of vision. Technical and scheduling limitations prevented pSD from completing adaptation rate testing.

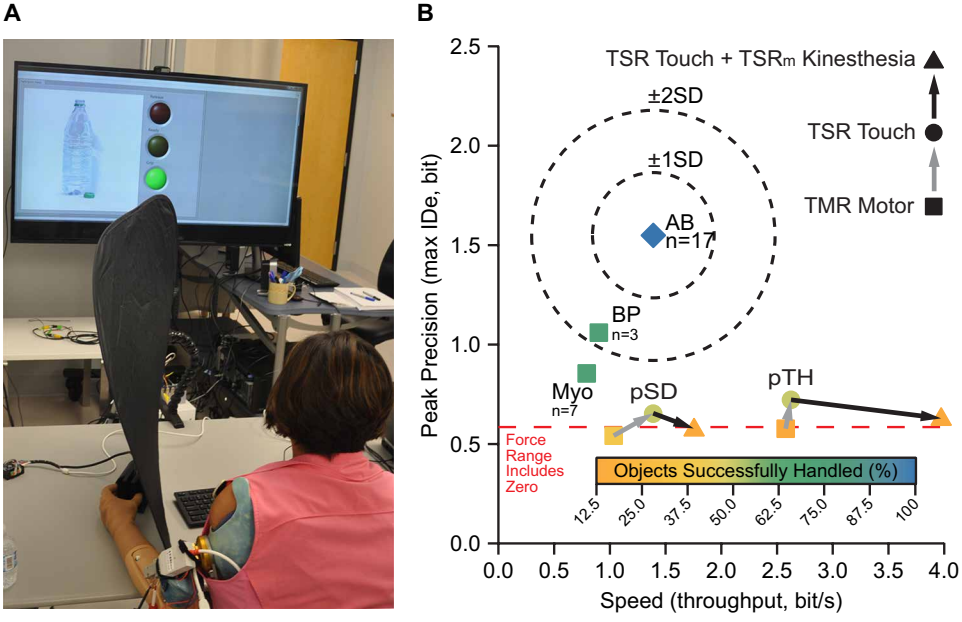

Fig. 6. Providing neurorobotic touch improves speed, precision, and number of objects successfully handled. (**A**) A participant performing the GRIP test. (**B**) This figure summarizes three test subscores, (i) percentage of objects successfully handled (gold to blue color gradient), (ii) peak precision of force generated (*y* axis), and (iii) the throughput, which describes the trade-off between speed and precision (*x* axis), where a higher value indicates that the user achieves any given precision faster, independent of the range of precision values that participants operated within. The results for each population [pSD and pTH (square to circle to triangle) and the body-powered (BP) and native myoelectric (Myo) prosthetic users (BP square and Myo square)] are compared with able-bodied performance (AB) (AB diamond). The movement on the plot resulting from the addition of TSR-touch to TMR-motor is shown as a gray arrow. The movement on the plot resulting from the addition of TSR_m-kinesthesia to TSR-touch and TMR-motor is shown as a black arrow. SD, SD able-bodied; IDe, effective index of difficulty.

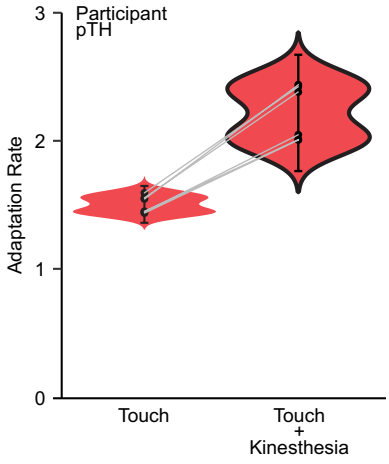

Fig. 7. Adaptation rate increases with neurorobotic kinesthesia and touch. Violin plots showing computed adaptation rate for pTH using the following: (i) equal number of trials, (ii) discarded first trial, (iii) discarded last trial, (iv) discarded first and last trials, (v) discarded last two trials, and (vi) discarded first two trial method. Trials were discarded to provide a measure of sensitivity (see text S5). The red shaded area represents the distribution of the calculated values of adaptation rate for pTH when receiving TSR-touch feedback. The red shaded area with the black outline represents the distribution of the calculated values of adaptation rate for pTH when receiving TSR_m-kinesthesia and TSR-touch feedback. The gray connecting lines show how each of these methods of calculating adaptation rate correspond for each feedback condition.

DISCUSSION

We are entering a phase of prosthetic development whereby accessing the neural system to return natural function is providing a pathway to improving performance. Standard-of-care prosthetic limbs require non-natural adaptive behaviors to compensate for the loss of a highly dexterous system (*45*, *46*, *70*). The goal for bionic prostheses is to access intrinsic neural communication channels to release the user from managing all the tasks and minutia required to pilot their devices (*71*). Returning sensory-motor channels would be anticipated to restore more natural behaviors to the human-machine system. However, quantifying the complexities of bionic sensory-motor integration is a nuanced proposition.

Neurally induced prosthetic sensation is a recent development (*4*). Many methods for quantifying interventional merit are either context-dependent or lag behind the technologies that they are attempting to assess. Our validated outcome measures represent an important step forward in assessing bionic sensory-motor interventions. By providing the resolution needed for evaluating human-machine interactions, our metrics reveal that bidirectional neurorobotic integration leads to more human-like function.

Organisms instinctively make strategic decisions about how to spend their resources in relationship to the payoff from their actions. Humans are subject to these same instincts (*72*–*75*), and PEP provides insight into resource allocation decisions made during sensory discrimination tasks (*49*, *50*). With TMR-motor only, pSD made discrimination decisions slightly above chance. With the ability to discriminate block stiffness through TSR-touch, pSD shifted strategy and improved system performance, striking a balance between making some mistakes for the sake of speed and slowing down to make more accurate discrimination decisions. With the addition of TSR-touch and TSR_m-kinesthesia to TMR-motor intent, pSD's decision strategy remained balanced, while her system performance improved to stratify with able-bodied participants. With TMR-motor control only, pTH's balanced decision strategy aligned with high-functioning native myoelectric users, likely relying on grip control and motor sound feedback to discern block stiffness (*76*). Although pTH started with high system performance and a balanced decision strategy, he showed improvement patterns similar to pSD. With each neurorobotic modality, pTH tracked along the balanced strategy curve to end at the apex of the standard-of-care prosthetic users and approaching able-bodied–type decision-making. If we were to look solely at pSD and pTH's time-focused performance, as is typical for standard-of-care metrics, these improvements and behaviors would be hidden.

We observed shifts to more able-bodied patterns in visual behaviors. Without sensation, prosthesis users gaze at their hand so that they do not miss, drop, or crush the objects they are grasping (*45*, *77*, *78*). Able-bodied behavior is to briefly look at an object to locate it for grasping and then focus attention on the location where they want to move it (*42*). With TSR-touch and TSR_m-kinesthesia, more normal visual behavior was restored for both pSD and pTH over TMR-motor alone. They spent significantly less time looking at their prosthetic hands during object transport. pSD's shift to freeing her gaze to look ahead to the next target of action was also evident during a more complex task involving reaching for a box outside her typical sphere of movement. The normalization of visuomotor behavior is a key requirement to allow accurate preplanning of movement strategies (*79*) and likely resulted from trusting TSR_m-kinesthesia and TSR-touch over visual compensation.

When integrating sensory information, the brain appears to assign levels of trust to the different inputs used to inform guidance and error correction of intended movements (*80*). Within this Bayesian perspective, higher informational content streams are trusted more and play a greater role in modifying the brain's representation and perception of this information (the internal model). Measurement of the participant's adaptation to intrinsic error can serve as a proxy to quantify internal model modification. With TSR-touch and TSR_m-kinesthesia, pTH showed an increased adaptation rate that reflected more trust in sensory inputs and a shift toward more natural intrinsic brain behaviors. These results align with literature, suggesting that kinesthetic feedback is a dominant modality in forming internal models (*81*, *82*).

The brain's sensory-motor comparative mechanisms drive the processes of movement error correction and experiential learning, and those same mechanisms compare sensation, vision, and intent to construct a cognitive sense of wholeness (*83*). The naturalness of sensation, the sensory modalities themselves, and the cohesiveness of sensory-motor fusion have critical roles in establishing limb ownership. Prostheses lacking neurally integrated feedback are excluded from the mechanisms of ownership (*62*, *84*). The Dynamic PIC test reveals a shift toward normal multisensory integration with neurorobotic systems. With TSR-touch alone, both pTH and pSD showed levels of limb ownership that were aligned with able-bodied responses to skin deformation. Restored touch appeared to be interpreted by the brain as similar to how sensation from native skin is interpreted. Corroborating questionnaire results in earlier work showed that TSR-touch provided a limb ownership sense as vivid as an able-bodied experience (*62*). These results reflect reactivation of appropriate tactile sensory channels in targeted reinnervation where psychophysical experiments showed restored skin mechanoreceptor

functionality (*58*, *59*). TSR-touch with TSR_m-kinesthesia further potentiated limb ownership for pTH, suggesting that visually observing active intentional movement potentiates ownership (*85*). Although pSD scored near intact physiology for prosthesis ownership with TSR-touch, adding TSR_m-kinesthesia reduced her Dynamic PIC score. Technical inconsistencies in pSD's kinesthetic feedback system appeared to influence the millisecond-level timing sensitivity of the brain's multisensory integration system, highlighting the resolution of Dynamic PIC as an assessment metric for evaluating the naturalness of bionic prostheses.

Kinesthetic and tactile information improved bionic prosthetic performance by multiple measures. However, if different sensation modalities are contextually or functionally misaligned, performance can be impaired. In the GRIP test, providing TSR-touch with TMR-motor control allowed pTH and pSD to improve their ability to successfully handle objects, which equates to generating an intermediate grasp force that is statistically distinct from their maximum force output (see fig. S5). Furthermore, those successfully handled objects were grasped with greater precision and speed. Introducing TSR_m-kinesthesia resulted in a loss of most of their small gains in precision compared with TSR-touch and returned the number of objects successfully handled to baseline. Although it is difficult to draw firm conclusions from the throughput because of the reduced number of objects successfully handled, with TSR_m-kinesthesia, both pSD and pTH appeared to improve the speed with which they interacted with the manipulandum (fig. S5, D to H). Because TSR_m-kinesthesia was likely affected by the incompressible manipulandum, it did not appear to provide the feedback necessary for effective sensory-motor integration. When applying precise grip force, a nonphysiological transition to losing TSR_m-kinesthesia when the hand movement stopped after contacting the manipulandum seemed disruptive for both pTH and pSD. These results were also reflected in the Dynamic PIC test for pSD and highlight the importance of feedback modality alignment. Revised approaches could decouple kinesthetic feedback from physical prosthetic movement, instead driving kinesthesia from intentional control signals or a hybrid of the two approaches. Redesigning the GRIP test with a compressible manipulandum or implementing compliant prosthetic fingers may also create a more widely applicable testing system.

Our functional metrics focused on distinct areas of integrated sensory-motor performance to highlight the roles that sensory feedback plays in adoption of natural behaviors. The metrics revealed a comprehensive and cohesive picture of more human-like function in bionic bidirectional prosthetic systems. Emerging technologies face critical roadblocks to clinical translation because of difficulties in demonstrating improvements over standard-of-care interventions. Although standard-of-care prostheses are functionally effective and relatively inexpensive, they have serious limitations. Body-powered and native myoelectric prostheses demand behavioral adaptations that alter attention and concentration and require abnormal body movements to operate (*45*, *46*, *77*, *78*, *86*). Prosthetic limb use is severely limited compared with normal limbs (*87*), leading to overuse and compensatory injuries (*88*, *89*) and risk of device abandonment (*90*). The goal of implementing sensate robotic prostheses is to overcome these barriers by introducing systems that allow more natural behaviors. Our metrics should be directly transferable to other bionic sensory-motor prosthetic systems and other upper limb sensory-motor deficits to provide a picture of where any approach resides on the continuum of severely impaired to the gold standard of able-bodied function. Studies of bidirectional bionic prosthetic systems could benefit from these standard benchmarks for comparison across approaches.

Study limitations and next steps

A study limitation was sample size. Only two participants with sensory-motor targeted reinnervation could commit to the long study period and intensive experimental time required. Limits on increasing the sample size arose from the necessity of international travel for the participants and research teams. Future studies may access more participants because targeted reinnervation is becoming limb amputation standard of care for prosthetic control, neuroma, and pain management (*91*, *92*).

pTH required control simplification (restricting elbow function) during a subset of tests. This is not an uncommon compensation of those with high-level amputation, and it simplified measuring the effects of sensory feedback modes. A coding bug was revealed in pSD's TSR_m-kinesthesia system during experiments. This problem was corrected, but the inflexible experimental schedule prevented retesting.

The challenges of overcoming technical limitations were offset by advantages from implementing the bionic systems with off-the-shelf prosthetic components. We did this for two principal reasons. The first was to provide evidence that performance improvements could be attributed to the quality of the neurorobotic sensory-motor information alone and not to the functionality of advanced mechatronics. The second was to evaluate the outcomes of bidirectionally integrated sensory-motor control within the real-world context of current prosthetic options.

Multiple touch and kinesthetic percepts were available for each participant. However, we chose to provide neurorobotic feedback for the most clinically and functionally relevant percepts (digit touch and grasp kinesthesia). Additional sensory locations and modalities could be considered given the number of available functions of emerging advanced mechatronic prosthetic systems.

Relating laboratory-based or clinical tests to daily life prosthesis use is challenging. Promising approaches use activity tracking and other in-home monitoring to quantify the amount, type, and complexity of prosthesis use (*87*, *93*). However, the factors that determine or influence use patterns remain an open question. To explore questions of capacity and performance in relation to gold standard normative behavior, we designed our metrics to involve more complex multimovement tasks (GaMA and PEP) and to challenge sensory-motor processing (GRIP, Dynamic PIC, and adaptation). Our tests quantify features of sensory-motor behavior and may provide insight into factors that influence daily life prosthesis use patterns.

MATERIALS AND METHODS

Study design

Participants previously underwent targeted reinnervation for proximal limb amputation. They were familiar with TMR myoelectric prosthesis use and had documented sensory percepts related to their missing limb (*31*). We fit each participant with an experimental prosthesis using modified commercial components that were integrated with myoelectric TMR-motor control and with feedback for TSR-touch and TSR_m-kinesthesia. There were three data collection conditions for each participant: TMR-motor control only and no sensory feedback, TSR-touch coupled with TMR-motor control, and TSR_m-kinesthesia and TSR-touch feedback coupled with TMR-motor

control. For each feedback/control condition, we administered PEP, GaMA, PIC, GRIP, and adaptation rate. Condition order randomization was not possible because of technical requirements and data collection scheduling limitations. Experiments were performed over 2 to 5 days of testing at the University of Alberta (GaMA, PIC, and adaptation rate) and Cleveland Clinic (GRIP/PEP) in 2018 to 2019.

Participants with amputation

pSD was a 38-year-old female with a left shoulder disarticulation who underwent targeted motor and sensory reinnervation of the chest muscles and skin (*56*). pTH was a 40-year-old male with a left transhumeral amputation who underwent targeted motor and sensory reinnervation of the upper arm muscles and skin. Participants provided written informed consent on study protocols approved by the Institutional Review Board of Cleveland Clinic (protocol #13-1349), the University of Alberta Health Research Ethics Board (Pro00054011 and Pro00066774), the University of New Brunswick Research Ethics Board (protocol #2015-033), the Department of the Navy Human Research Protection Program (DON-HRPP), and the Space and Naval Warfare Systems Center Pacific Human Research Protection Office (SSCPAC HRPO).

Neuromotor control

The system for intentional motor control used surface electromyography to access the original arm control signals from the brain through contraction of neurally reassigned muscle sites. pSD operated four independent muscle sites for hand open/close and elbow flexion/extension of her reinnervated chest muscles from median, ulnar, musculocutaneous, and distal radial nerve transfers (*55*). She pressed force-sensitive resistor switches with her remnant humerus to control wrist rotation. pTH used reinnervated medial biceps (median nerve) and reinnervated lateral triceps (radial nerve) for hand open/close and native lateral biceps and triceps signals to operate elbow flexion/extension.

Neurorobotic touch

The neurorobotic touch feedback system sensed contact transients and pressure on the prosthesis in six different locations on the fingers and palm (*9*). The thumb, index, and middle fingers of a SensorHand Speed (Ottobock, Duderstadt, Germany) were milled and retrofitted with strain gauges to detect finger flexing from touch pressure. Force-sensitive resistors in the hand shell provided touch for the ring and little fingers and palm. Touch signals were internally routed to a processing unit (HDT Global, Fredericksburg, VA, USA) mounted on the internal frame of the SensorHand. Communication, control, diagnostics, system tuning, and reprogramming feedback modes ran via a Controller Area Network (CAN bus) through a custom six-channel rotating wrist. Small ruggedized robotic four-bar haptic touch tactors (HDT Global, Fredericksburg, VA, USA) were mounted to the prosthetic socket and relayed proportional pressure and contact transients (tap detection) from the hand to the appropriate touch percept sites in the reinnervated skin. The touch tactors could generate up to 10 N of force and operated on a 10-ms latency closed-loop position control that rapidly adjusted motor effort for correct pressure and position against the skin. Verbal feedback was used to adjust the touch feedback until the participant felt that it was appropriate. pSD preferred combined proportional pressure and tap detection modes together, whereas pTH preferred proportional mode.

Neurorobotic kinesthesia

The neurorobotic kinesthetic feedback system detected the physical movement of hand closing through a Bowden cable spanning the prosthetic thumb and distal wrist that connected to a cable-extension transducer mounted at the shoulder. When the prosthetic hand closed, the potentiometer signal was used to activate a small robotic kinesthetic tactor (HDT Global, Fredericksburg, VA, USA) that vibrated the reinnervated deep muscle at 90 Hz (1-mm stroke) through a hole in the prosthetic socket. The vibration elicited the sensation of hand closing at deep muscle locations that were determined for each participant (*31*). The kinesthetic tactor autoretracted during donning and doffing and during periods of inactivity between experimental blocks. A 10-ms system response time allowed the kinesthetic tactor to modulate motor effort while maintaining the 1-mm stroke against the resistance of the deep muscle to minimize delay between hand movement and kinesthetic sensation.

Prosthesis Efficiency and Profitability (PEP)

The PEP task required participants to find and remove five blocks of a target stiffness (either soft or hard) among distractors (i.e., a soft target among medium and hard distractors or a hard target among soft and medium distractors) as quickly and accurately as possible (*49*). We recorded the number of blocks squeezed (encounters), the number of correct blocks selected, and the trial duration. Participants completed 150 rubber block selections (50 soft, 50 hard, and 50 baseline) per test condition (see text S1 for detailed methods). Each trial was divided into three analysis subsections: search time, the time required to locate the block that was ultimately selected; involvement time, the time spent discriminating stiffness and transporting the block that was selected; and handling time, the time spent grasping and transporting blocks during nondiscriminating baseline trials. Values extracted from this information were recognition time, accuracy, false-positive rate and false-negative rate, and efficiency. Determination of significance was done with z tests of proportion for accuracy, Wilcoxon rank sum tests for search times, and t tests for recognition and handling times. A significance level of 0.05 was used for all tests.

Gaze and Movement Assessment (GaMA)

Participants performed the cup transfer task detailed in the work of Valevicius *et al.* (*41*). An eight-camera OptiTrack Flex 13 motion capture system (Natural Point, OR, USA) captured the three-dimensional trajectories of motion capture markers affixed to the participants and task and environment (*40*, *41*). A Pupil Labs head-mounted binocular eye tracker (Pupil Labs GmbH, Berlin, Germany) captured pupil position (*44*). Before the task, the participants were provided verbal instructions, a demonstration, and as many practice trials as needed to feel comfortable (table S2). The motion capture and eye tracking data were cleaned, filtered, synchronized, and segmented into reach, grasp, transport, and release phases. A gaze vector representing the virtual location of each participant's gaze in the coordinate frame of the motion tracked objects was created with a regression function using custom MATLAB scripts (*41*, *42*). Main outcomes in the reach and transport phases were percent fixations to the prosthetic hand and to the current area of action (see text S2 for detailed methods and analysis). Differences between the three conditions (TMR-motor, TSR-touch, and TSR_m-kinesthesia + TSR-touch) were analyzed using a one-way analysis of variance and post hoc tests. Assumptions of normality and homogeneity

of variances in each group were tested using Shapiro-Wilk's test and Levene's test for equality of variance.

Dynamic Prosthesis Incorporation (PIC)

Crossmodel congruency was used to evaluate prosthesis ownership by assessing the ability to ignore one form of feedback in favor of another (*51*). Participants had green light-emitting diodes (LEDs) affixed to the prosthetic thumb and index finger at locations corresponding to thumb and index touch percepts. A distractor LED was affixed to a load cell, halfway between the thumb and index of the prosthesis. The participants dynamically grasped an instrumented object with the thumb and fingers of their prosthesis. Their forearm was secured with Velcro to a mount to assure simultaneous activation of touch percepts when contacting the instrumented object. Under all conditions, touch feedback and LED light feedback were provided at one of the two stimulation sites when the participant made contact with the object, with kinesthetic feedback of hand closing provided during a subset of trials. After grasping the instrumented object, the participants indicated which touch tactor had been activated by pressing a corresponding foot pedal (heel pedal, thumb and toe pedal, index finger). The average congruent and incongruent time for each block was calculated after participants completed 30 practice trials and four testing blocks of 64 trials (see text S2 for detailed methods and analysis). The difference between congruent and incongruent time was taken, and then the average difference across blocks was calculated. This value was converted into a PIC score that reveals the effects of spatial discrepancies between visual representation and stimulation representation (*52*).

Grasping Relative Index of Performance (GRIP)

Participants sat at a table facing a monitor, with their prosthetic hand at a grasp force–measuring manipulandum and their able-bodied hand at a keyboard. Participants were shown images of eight different everyday objects on the monitor (fig. S5A) (*47*). They were instructed to grasp the manipulandum with a force that they thought was sufficient to lift the displayed object without crushing or damaging it and to be both fast and accurate while attempting one single grasp before moving to the next trial. Object order was pseudo-randomized and presented in blocks of 32 trials, with a total of 160 trials in each feedback condition (see text S4 for details). We calculated an IDe for each object (*47*), which describes the ratio of the average peak force to trial-to-trial force variability (higher forces produced with less variability describe the handling of a more difficult object). We calculated three measures: objects successfully handled, peak precision, and speed (*9*, *47*). Objects successfully handled was a measure of how reliably a participant could produce intermediate forces. Peak precision was the highest IDe of successful objects in either the standard or "precision" blocks. Speed (or throughput, in bits per second) was the average inverse slope of time and IDe for successfully handled objects in the standard, timed (nonprecision) task.

Adaptation rate

We used trial-by-trial adaptation rate to evaluate how individuals adapt on the next trial, given what happened on the current trial (*94*, *95*). Adaptation rate is defined as the ratio between trial-to-trial change and trial error

$$\text{Adaptation rate} = \frac{x^{k+1} - x^{k}}{x^{k} - x_T}$$

where x is the position, superscript index ^{k} denotes a given trial number, and x_T denotes the target position. We expanded on this definition by considering additional position states. In this experiment, we used TSR-touch feedback and the same TMR-motor control under both conditions with one of these conditions serving as a baseline. Under a second condition, we asked whether augmenting the system with TSR_m-kinesthesia added value compared with vision alone. In the test, the participant sat in a chair with his prosthetic arm on the table and was asked to use his prosthetic hand to catch a falling vertical bar at a target located halfway along its length. The vertical bar's fall was coupled to a pulley system operated by an experimenter (fig. S6), and its position was recorded using an array of Hall effect sensors. Participants completed a practice block of 35 trials and then a testing block of 35 trials with their error recorded for each trial (see text S5 for detailed methods and analysis).

SUPPLEMENTARY MATERIALS

robotics.sciencemag.org/cgi/content/full/6/58/eabf3368/DC1
Texts S1 to S5
Figs. S1 to S6
Tables S1 to S6
References (*97*–*99*)

REFERENCES AND NOTES

1. D. Farina, N. Jiang, H. Rehbaum, A. Holobar, B. Graimann, H. Dietl, O. C. Aszmann, The extraction of neural information from the surface EMG for the control of upper-limb prostheses: Emerging avenues and challenges. *IEEE Trans. Neural Syst. Rehabil. Eng. A* **22**, 797–809 (2014).
2. K. A. Yildiz, A. Y. Shin, K. R. Kaufman, Interfaces with the peripheral nervous system for the control of a neuroprosthetic limb: A review. *J. Neuroeng. Rehabil.* **17**, 43 (2020).
3. M. Vilela, L. R. Hochberg, Applications of brain-computer interfaces to the control of robotic and prosthetic arms. *Handb. Clin. Neurol.* **168**, 87–99 (2020).
4. S. J. Bensmaia, D. J. Tyler, S. Micera, Restoration of sensory information via bionic hands. *Nat. Biomed. Eng.* (2020).
5. J. W. Sensinger, S. Dosen, A review of sensory feedback in upper-limb prostheses from the perspective of human motor control. *Front. Neurosci.* **14**, 345 (2020).
6. S. Raspopovic, A. Cimolato, A. Panarese, F. Vallone, J. Del Valle, S. Micera, X. Navarro, Neural signal recording and processing in somatic neuroprosthetic applications. A review. *J. Neurosci. Methods* **337**, 108653 (2020).
7. P. Svensson, U. Wijk, A. Björkman, C. Antfolk, A review of invasive and non-invasive sensory feedback in upper limb prostheses. *Expert Rev. Med. Devices* **14**, 439–447 (2017).
8. M. Ortiz-Catalan, E. Mastinu, P. Sassu, O. Aszmann, R. Brånemark, Self-contained neuromusculoskeletal arm prostheses. *N. Engl. J. Med.* **382**, 1732–1738 (2020).
9. J. S. Schofield, C. E. Shell, D. T. Beckler, Z. C. Thumser, P. D. Marasco, Long-term home-use of sensory-motor-integrated bidirectional bionic prosthetic arms promotes functional, perceptual, and cognitive changes. *Front. Neurosci.* **14**, 120 (2020).
10. F. Clemente, G. Valle, M. Controzzi, I. Strauss, F. Iberite, T. Stieglitz, G. Granata, P. M. Rossini, F. Petrini, S. Micera, C. Cipriani, Intraneural sensory feedback restores grip force control and motor coordination while using a prosthetic hand. *J. Neural Eng.* **16**, 026034 (2019).
11. L. Cappello, W. Alghilan, M. Gabardi, D. Leonardis, M. Barsotti, A. Frisoli, C. Cipriani, Continuous supplementary tactile feedback can be applied (and then removed) to enhance precision manipulation. *J. Neuroeng. Rehabil.* **17**, 120 (2020).
12. E. Mastinu, L. F. Engels, F. Clemente, M. Dione, P. Sassu, O. Aszmann, R. Brånemark, B. Håkansson, M. Controzzi, J. Wessberg, C. Cipriani, M. Ortiz-Catalan, Neural feedback strategies to improve grasping coordination in neuromusculoskeletal prostheses. *Sci. Rep.* **10**, 11793 (2020).
13. A. M. De Nunzio, S. Dosen, S. Lemling, M. Markovic, M. A. Schweisfurth, N. Ge, B. Graimann, D. Falla, D. Farina, Tactile feedback is an effective instrument for the training of grasping with a prosthesis at low- and medium-force levels. *Exp. Brain Res.* **235**, 2547–2559 (2017).
14. D. W. Tan, M. A. Schiefer, M. W. Keith, J. R. Anderson, J. Tyler, D. J. Tyler, A neural interface provides long-term stable natural touch perception. *Sci. Transl. Med.* **6**, 257ra138 (2014).
15. G. S. Dhillon, K. W. Horch, Direct neural sensory feedback and control of a prosthetic arm. *IEEE Trans. Neural Syst. Rehabil. Eng.* **13**, 468–472 (2005).
16. K. Kim, J. E. Colgate, Haptic feedback enhances grip force control of sEMG-controlled prosthetic hands in targeted reinnervation amputees. *IEEE Trans. Neural Syst. Rehabil. Eng. A* **20**, 798–805 (2012).

17. M. Štrbac, M. Isaković, M. Belić, I. Popović, I. Simanić, D. Farina, T. Keller, S. Došen, Short- and long-term learning of feedforward control of a myoelectric prosthesis with sensory feedback by amputees. *IEEE Trans. Neural Syst. Rehabil. Eng.* **25**, 2133–2145 (2017).
18. G. Valle, A. Mazzoni, F. Iberite, E. D'Anna, I. Strauss, G. Granata, M. Controzzi, F. Clemente, G. Rognini, C. Cipriani, T. Stieglitz, F. M. Petrini, P. M. Rossini, S. Micera, Biomimetic intraneural sensory feedback enhances sensation naturalness, tactile sensitivity, and manual dexterity in a bidirectional prosthesis. *Neuron* **100**, 37–45.e7 (2018).
19. E. D'Anna, G. Valle, A. Mazzoni, I. Strauss, F. Iberite, J. Patton, F. M. Petrini, S. Raspopovic, G. Granata, R. Di Iorio, M. Controzzi, C. Cipriani, T. Stieglitz, P. M. Rossini, S. Micera, A closed-loop hand prosthesis with simultaneous intraneural tactile and position feedback. *Sci. Robot.* **4**, eaau8892 (2019).
20. C. Cipriani, J. L. Segil, F. Clemente, R. F. ff Weir, B. Edin, Humans can integrate feedback of discrete events in their sensorimotor control of a robotic hand. *Exp. Brain Res.* **232**, 3421–3429 (2014).
21. D. Farina, I. Vujaklija, R. Brånemark, A. M. J. Bull, H. Dietl, B. Graimann, L. J. Hargrove, K.-P. Hoffmann, H. Huang, T. Ingvarsson, H. B. Janusson, K. Kristjánsson, T. Kuiken, S. Micera, T. Stieglitz, A. Sturma, D. Tyler, R. F. ff Weir, O. C. Aszmann, Toward higher-performance bionic limbs for wider clinical use. *Nat. Biomed. Eng.* (2021).
22. F. W. Clippinger, R. Avery, B. R. Titus, A sensory feedback system for an upper-limb amputation prosthesis. *Bull. Prosthet. Res.* 247–258 (1974).
23. J. A. George, D. T. Kluger, T. S. Davis, S. M. Wendelken, E. V. Okorokova, Q. He, C. C. Duncan, D. T. Hutchinson, Z. C. Thumser, D. T. Beckler, P. D. Marasco, S. J. Bensmaia, G. A. Clark, Biomimetic sensory feedback through peripheral nerve stimulation improves dexterous use of a bionic hand. *Sci. Robot.* **4**, eaax2352 (2019).
24. M. A. Schiefer, E. L. Graczyk, S. M. Sidik, D. W. Tan, D. J. Tyler, Artificial tactile and proprioceptive feedback improves performance and confidence on object identification tasks. *PLOS ONE* **13**, e0207659 (2018).
25. K. Horch, S. Meek, T. G. Taylor, D. T. Hutchinson, Object discrimination with an artificial hand using electrical stimulation of peripheral tactile and proprioceptive pathways with intrafascicular electrodes. *IEEE Trans. Neural Syst. Rehabil. Eng.* **19**, 483–489 (2011).
26. J. L. Segil, I. Cuberovic, E. L. Graczyk, R. F. ff Weir, D. Tyler, Combination of simultaneous artificial sensory percepts to identify prosthetic hand postures: A case study. *Sci. Rep.* **10**, 6576 (2020).
27. I. Cuberovic, A. Gill, L. J. Resnik, D. J. Tyler, E. L. Graczyk, Learning of artificial sensation through long-term home use of a sensory-enabled prosthesis. *Front. Neurosci.* **13**, 853 (2019).
28. S. Wendelken, D. M. Page, T. Davis, H. A. C. Wark, D. T. Kluger, C. Duncan, D. J. Warren, D. T. Hutchinson, G. A. Clark, Restoration of motor control and proprioceptive and cutaneous sensation in humans with prior upper-limb amputation via multiple Utah Slanted Electrode Arrays (USEAs) implanted in residual peripheral arm nerves. *J. Neuroeng. Rehabil.* **14**, 121 (2017).
29. T. R. Clites, M. J. Carty, S. S. Srinivasan, S. G. Talbot, R. Brånemark, H. M. Herr, Caprine models of the agonist-antagonist myoneural interface implemented at the above- and below-knee amputation levels. *Plast. Reconstr. Surg.* **144**, 218e–229e (2019).
30. S. S. Srinivasan, S. Gutierrez-Arango, A. C.-E. Teng, E. Israel, H. Song, Z. K. Bailey, M. J. Carty, L. E. Freed, H. M. Herr, Neural interfacing architecture enables enhanced motor control and residual limb functionality postamputation. *Proc. Natl. Acad. Sci. U.S.A.* **118**, e2019555118 (2021).
31. P. D. Marasco, J. S. Hebert, J. W. Sensinger, C. E. Shell, J. S. Schofield, Z. C. Thumser, R. Nataraj, D. T. Beckler, M. R. Dawson, D. H. Blustein, S. Gill, B. D. Mensh, R. Granja-Vazquez, M. D. Newcomb, J. P. Carey, B. M. Orzell, Illusory movement perception improves motor control for prosthetic hands. *Sci. Transl. Med.* **10**, eaao6990 (2018).
32. W. Hill, P. Kyberd, L. Norling Hermansson, S. Hubbard, Ø. Stavdahl, S. Swanson, Upper Limb Prosthetic Outcome Measures (ULPOM): A working group and their findings. *J. Prosthetics Orthot.* **21**, P69–P82 (2009).
33. H. Y. Lindner, B. S. Natterlund, L. M. Hermansson, Upper limb prosthetic outcome measures: Review and content comparison based on International Classification of Functioning, Disability and Health. *Prosthetics Orthot. Int.* **34**, 109–128 (2010).
34. L. Resnik, M. Borgia, B. Silver, J. Cancio, Systematic review of measures of impairment and activity limitation for persons with upper limb trauma and amputation. *Arch. Phys. Med. Rehabil.* **98**, 1863–1892.e14 (2017).
35. S. Wang, C. J. Hsu, L. Trent, T. Ryan, N. T. Kearns, E. F. Civillico, K. L. Kontson, Evaluation of performance-based outcome measures for the upper limb: A comprehensive narrative review. *PM R* **10**, 951–962.e3 (2018).
36. M. Markovic, M. A. Schweisfurth, L. F. Engels, T. Bentz, D. Wüstefeld, D. Farina, S. Dosen, The clinical relevance of advanced artificial feedback in the control of a multi-functional myoelectric prosthesis. *J. Neuroeng. Rehabil.* **15**, 28 (2018).
37. A. W. Shehata, L. F. Engels, M. Controzzi, C. Cipriani, E. J. Scheme, J. W. Sensinger, Improving internal model strength and performance of prosthetic hands using augmented feedback. *J. Neuroeng. Rehabil.* **15**, 70 (2018).
38. S. Gill, A. Wilson, D. Blustein, J. Sensinger, The crossmodal congruency effect, a tool incorporation metric, suffers from a learning effect with repeated exposures. *bioRxiv*, 186825 (2017).
39. A. M. Valevicius, P. Y. Jun, J. S. Hebert, A. H. Vette, Use of optical motion capture for the analysis of normative upper body kinematics during functional upper limb tasks: A systematic review. *J. Electromyogr. Kinesiol.* **40**, 1–15 (2018).
40. Q. A. Boser, A. M. Valevicius, E. B. Lavoie, C. S. Chapman, P. M. Pilarski, J. S. Hebert, A. H. Vette, Cluster-based upper body marker models for three-dimensional kinematic analysis: Comparison with an anatomical model and reliability analysis. *J. Biomech.* **72**, 228–234 (2018).
41. A. M. Valevicius, Q. A. Boser, E. B. Lavoie, G. S. Murgatroyd, P. M. Pilarski, C. S. Chapman, A. H. Vette, J. S. Hebert, Characterization of normative hand movements during two functional upper limb tasks. *PLOS ONE* **13**, e0199549 (2018).
42. E. B. Lavoie, A. M. Valevicius, Q. A. Boser, O. Kovic, A. H. Vette, P. M. Pilarski, J. S. Hebert, C. S. Chapman, Using synchronized eye and motion tracking to determine high-precision eye-movement patterns during object-interaction tasks. *J. Vis.* **18**, 18 (2018).
43. A. M. Valevicius, Q. A. Boser, E. B. Lavoie, C. S. Chapman, P. M. Pilarski, J. S. Hebert, A. H. Vette, Characterization of normative angular joint kinematics during two functional upper limb tasks. *Gait Posture* **69**, 176–186 (2019).
44. H. E. Williams, C. S. Chapman, P. M. Pilarski, A. H. Vette, J. S. Hebert, Gaze and Movement Assessment (GaMA): Inter-site validation of a visuomotor upper limb functional protocol. *PLOS ONE* **14**, e0219333 (2019).
45. J. Hebert, Q. Boser, A. Valevicius, H. Tanikawa, E. Lavoie, A. Vette, P. Pilarski, C. Chapman, Quantitative eye gaze and movement differences in visuomotor adaptations to varying task demands among upper-extremity prosthesis users. *JAMA Netw. Open* **2**, e1911197 (2019).
46. A. M. Valevicius, Q. A. Boser, C. S. Chapman, P. M. Pilarski, A. H. Vette, J. S. Hebert, Compensatory strategies of body-powered prosthesis users reveal primary reliance on trunk motion and relation to skill level. *Clin. Biomech.* **72**, 122–129 (2020).
47. Z. C. Thumser, A. B. Slifkin, D. T. Beckler, P. D. Marasco, Fitts' law in the control of isometric grip force with naturalistic targets. *Front. Psychol.* **9**, 560 (2018).
48. J. E. Downey, J. M. Weiss, S. N. Flesher, Z. C. Thumser, P. D. Marasco, M. L. Boninger, R. A. Gaunt, J. L. Collinger, Implicit grasp force representation in human motor cortical recordings. *Front. Neurosci.* **12**, 801 (2018).
49. D. T. Beckler, Z. C. Thumser, J. S. Schofield, P. D. Marasco, Using sensory discrimination in a foraging-style task to evaluate human upper-limb sensorimotor performance. *Sci. Rep.* **9**, 5806 (2019).
50. D. T. Beckler, Z. C. Thumser, J. S. Schofield, P. D. Marasco, Reliability in evaluator-based tests: Using simulation-constructed models to determine contextually relevant agreement thresholds. *BMC Med. Res. Methodol.* **18**, 141 (2018).
51. D. Blustein, A. Shehata, K. Englehart, J. Sensinger, Conventional analysis of trial-by-trial adaptation is biased: Empirical and theoretical support using a Bayesian estimator. *PLoS Comput. Biol.* **14**, e1006501 (2018).
52. D. Blustein, A. Wilson, J. Sensinger, Assessing the quality of supplementary sensory feedback using the crossmodal congruency task. *Sci. Rep.* **8**, 6203 (2018).
53. A. W. Shehata, E. J. Scheme, J. W. Sensinger, Evaluating internal model strength and performance of myoelectric prosthesis control strategies. *IEEE Trans. Neural Syst. Rehabil. Eng.* **26**, 1046–1055 (2018).
54. A. W. Shehata, E. J. Scheme, J. W. Sensinger, Audible feedback improves internal model strength and performance of myoelectric prosthesis control. *Sci. Rep.* **8**, 8541 (2018).
55. T. A. Kuiken, L. A. Miller, R. D. Lipschutz, B. A. Lock, K. Stubblefield, P. D. Marasco, P. Zhou, G. A. Dumanian, Targeted reinnervation for enhanced prosthetic arm function in a woman with a proximal amputation: A case study. *Lancet* **369**, 371–380 (2007).
56. T. A. Kuiken, P. D. Marasco, B. A. Lock, R. N. Harden, J. P. Dewald, Redirection of cutaneous sensation from the hand to the chest skin of human amputees with targeted reinnervation. *Proc. Natl. Acad. Sci. U.S.A.* **104**, 20061–20066 (2007).
57. J. S. Hebert, K. Elzinga, K. M. Chan, J. L. Olson, M. J. Morhart, Updates in targeted sensory reinnervation for upper limb amputation. *Curr. Surg. Rep.* **2**, 45–53 (2014).
58. A. E. Schultz, P. D. Marasco, T. A. Kuiken, Vibrotactile detection thresholds for chest skin of amputees following targeted reinnervation surgery. *Brain Res.* **1251**, 121–129 (2009).
59. P. D. Marasco, A. E. Schultz, T. A. Kuiken, Sensory capacity of reinnervated skin after redirection of amputated upper limb nerves to the chest. *Brain* **132**, 1441–1448 (2009).
60. J. S. Hebert, K. M. Chan, M. R. Dawson, Cutaneous sensory outcomes from three transhumeral targeted reinnervation cases. *Prosthetics Orthot. Int.* **40**, 303–310 (2016).
61. J. S. Hebert, J. L. Olson, M. J. Morhart, M. R. Dawson, P. D. Marasco, T. A. Kuiken, K. M. Chan, Novel targeted sensory reinnervation technique to restore functional hand sensation after transhumeral amputation. *IEEE Trans. Neural Syst. Rehabil. Eng.* **22**, 765–773 (2014).
62. P. D. Marasco, K. Kim, J. E. Colgate, M. A. Peshkin, T. A. Kuiken, Robotic touch shifts perception of embodiment to a prosthesis in targeted reinnervation amputees. *Brain* **134**, 747–758 (2011).
63. Human-robotic interfaces to shape the future of prosthetics. *EBioMedicine* **46**, 1 (2019).

64. E. L. Graczyk, L. Resnik, M. A. Schiefer, M. S. Schmitt, D. J. Tyler, Home use of a neural-connected sensory prosthesis provides the functional and psychosocial experience of having a hand again. *Sci. Rep.* **8**, 9866 (2018).
65. G. Rognini, F. M. Petrini, S. Raspopovic, G. Valle, G. Granata, I. Strauss, M. Solcà, J. Bello-Ruiz, B. Herbelin, R. Mange, E. D'Anna, R. Di Iorio, G. Di Pino, D. Andreu, D. Guiraud, T. Stieglitz, P. M. Rossini, A. Serino, S. Micera, O. Blanke, Multisensory bionic limb to achieve prosthesis embodiment and reduce distorted phantom limb perceptions. *J. Neurol. Neurosurg. Psychiatry* **90**, 833–836 (2019).
66. D. M. Page, J. A. George, D. T. Kluger, C. Duncan, S. Wendelken, T. Davis, D. T. Hutchinson, G. A. Clark, Motor control and sensory feedback enhance prosthesis embodiment and reduce phantom pain after long-term hand amputation. *Front. Hum. Neurosci.* **12**, 352 (2018).
67. F. M. Petrini, G. Valle, M. Bumbasirevic, F. Barberi, D. Bortolotti, P. Cvancara, A. Hiairrassary, P. Mijovic, A. Ö. Sverrisson, A. Pedrocchi, J.-L. Divoux, I. Popovic, K. Lechler, B. Mijovic, D. Guiraud, T. Stieglitz, A. Alexandersson, S. Micera, A. Lesic, S. Raspopovic, Enhancing functional abilities and cognitive integration of the lower limb prosthesis. *Sci. Transl. Med.* **11**, eaav8939 (2019).
68. E. L. Graczyk, A. Gill, D. J. Tyler, L. J. Resnik, M. Pazzaglia, The benefits of sensation on the experience of a hand: A qualitative case series. *PLOS ONE* **14**, e0211469 (2019).
69. K. Wei, K. Körding, Uncertainty of feedback and state estimation determines the speed of motor adaptation. *Front. Comput. Neurosci.* **4**, 11 (2010).
70. M. J. Major, R. L. Stine, C. W. Heckathorne, S. Fatone, S. A. Gard, Comparison of range-of-motion and variability in upper body movements between transradial prosthesis users and able-bodied controls when executing goal-oriented tasks. *J. Neuroeng. Rehabil.* **11**, 132–142 (2014).
71. T. R. Makin, F. de Vignemont, A. A. Faisal, Neurocognitive barriers to the embodiment of technology. *Nat. Biomed. Eng.* **1**, 0014 (2017).
72. M. Dwairy, A. C. Dowell, J.-C. Stahl, The application of foraging theory to the information searching behaviour of general practitioners. *BMC Fam. Pract.* **12**, 90 (2011).
73. P. E. Sandstrom, Scholars as subsistence foragers. *Bull. Am. Soc. Inf. Sci. Technol.* **25**, 17–20 (1999).
74. W. B. Whalley, Evaluating student assessments: The use of optimal foraging theory. *Assess. Eval. High. Educ.* **41**, 183–198 (2016).
75. M. Fielding, V. Jones, 'Disrupting the Optimal Forager': Predictive risk mapping and domestic burglary reduction in Trafford, Greater Manchester. *Int. J. Police Sci. Manag.* **14**, 30–41 (2012).
76. D. H. Silcox III, M. D. Rooks, R. R. Vogel, L. L. Fleming, Myoelectric prostheses. A long-term follow-up and a study of the use of alternate prostheses. *JBJS* **75**, 1781–1789 (1993).
77. M. M. D. Sobuh, L. P. J. Kenney, A. J. Galpin, S. B. Thies, J. M. Laughlin, J. Kulkarni, P. Kyberd, Visuomotor behaviours when using a myoelectric prosthesis. *J. Neuroeng. Rehabil.* **11**, 72 (2014).
78. J. V. V. Parr, S. J. Vine, N. R. Harrison, G. Wood, Examining the spatiotemporal disruption to gaze when using a myoelectric prosthetic hand. *J. Mot. Behav.* **50**, 416–425 (2018).
79. F. R. Sarlegna, P. K. Mutha, The influence of visual target information on the online control of movements. *Vis. Res.* **110**, 144–154 (2015).
80. M. O. Ernst, M. S. Banks, Humans integrate visual and haptic information in a statistically optimal fashion. *Nature* **415**, 429–433 (2002).
81. J. W. Krakauer, M.-F. Ghilardi, C. Ghez, Independent learning of internal models for kinematic and dynamic control of reaching. *Nat. Neurosci.* **2**, 1026–1031 (1999).
82. J. R. Lackner, P. Dizio, Rapid adaptation to Coriolis force perturbations of arm trajectory. *J. Neurophysiol.* **72**, 299–313 (1994).
83. O. Blanke, M. Slater, A. Serino, Behavioral, neural, and computational principles of bodily self-consciousness. *Neuron* **88**, 145–166 (2015).
84. H. H. Ehrsson, in *The New Handbook of Multisensory Processes*, B. Stein, Ed. (MIT Press, 2012), pp. 775–792.
85. A. Kalckert, H. H. Ehrsson, The onset time of the ownership sensation in the moving rubber hand illusion. *Front. Psychol.* **8**, 344 (2017).
86. S. L. Carey, M. Jason Highsmith, M. E. Maitland, R. V. Dubey, Compensatory movements of transradial prosthesis users during common tasks. *Clin. Biomech.* **23**, 1128–1135 (2008).
87. A. Chadwell, L. Kenney, M. H. Granat, S. Thies, J. Head, A. Galpin, R. Baker, J. Kulkarni, Upper limb activity in myoelectric prosthesis users is biased towards the intact limb and appears unrelated to goal-directed task performance. *Sci. Rep.* **8**, 11084 (2018).
88. C. R. Gambrell, Overuse syndrome and the unilateral upper limb amputee: Consequences and prevention. *JPO J. Prosthetics Orthot.* **20**, 126–132 (2008).
89. K. Ostlie, R. J. Franklin, O. H. Skjeldal, A. Skrondal, P. Magnus, Musculoskeletal pain and overuse syndromes in adult acquired major upper-limb amputees. *Arch. Phys. Med. Rehabil.* **92**, 1967–1973.e1 (2011).
90. L. Resnik, M. Borgia, S. Biester, M. A. Clark, Longitudinal study of prosthesis use in veterans with upper limb amputation. *Prosthetics Orthot. Int.* 0309364620957920 (2020).
91. T. A. Kuiken, A. K. Barlow, L. Hargrove, G. A. Dumanian, Targeted muscle reinnervation for the upper and lower extremity. *Tech. Orthop.* **32**, 109–116 (2017).
92. G. A. Dumanian, B. K. Potter, L. M. Mioton, J. H. Ko, J. E. Cheesborough, J. M. Souza, W. J. Ertl, S. M. Tintle, G. P. Nanos, I. L. Valerio, T. A. Kuiken, A. V. Apkarian, K. Porter, S. W. Jordan, Targeted muscle reinnervation treats neuroma and phantom pain in major limb amputees: A randomized clinical trial. *Ann. Surg.* **270**, 238–246 (2019).
93. A. J. Spiers, L. Resnik, A. M. Dollar, Analyzing at-home prosthesis use in unilateral upper-limb amputees to inform treatment & device design. *IEEE Int. Conf. Rehabil. Robot.* **2017**, 1273–1280 (2017).
94. L. Resnik, L. Adams, M. Borgia, J. Delikat, R. Disla, C. Ebner, L. S. Walters, Development and evaluation of the activities measure for upper limb amputees. *Arch. Phys. Med. Rehabil.* **94**, 488–494.e4 (2013).
95. L. Hermansson, A. Fisher, B. Bernspång, A. C. Eliasson, Assessment of capacity for myoelectric control: A new Rasch-built measure of prosthetic hand control. *J. Rehabil. Med.* **37**, 166–171 (2005).
96. A. W. Shehata, E. J. Scheme, J. W. Sensinger, in *2017 International Conference on Rehabilitation Robotics (ICORR)* (2017), pp. 200–204.
97. M. A. Conditt, F. Gandolfo, F. A. Mussa-Ivaldi, The motor system does not learn the dynamics of the arm by rote memorization of past experience. *J. Neurophysiol.* **78**, 554–560 (1997).
98. A. J. Bastian, Understanding sensorimotor adaptation and learning for rehabilitation. *Curr. Opin. Neurol.* **21**, 628–633 (2008).
99. D. Blustein, S. Gill, A. Wilson, J. Sensinger, Crossmodal congruency effect scores decrease with repeat test exposure. *PeerJ* **7**, e6976 (2019).

Acknowledgments: We thank J. Schofield, C. Shell, M. (Rory) Dawson, C. Chapman, M. Rehani, D. Blustein, Arm Dynamics, J. Kerbo, and E. Baron. **Funding:** This work was supported by the Defense Advanced Research Projects Agency (DARPA) Biological Technologies Office (BTO) under the auspices of D. Weber and A. Emondi through the DARPA Contracts Management Office Grant/Contract No. N66001-15-C-4015. H.E.W. was supported by the Alberta Innovates Graduate Student Scholarship and the Natural Sciences and Engineering Research Council of Canada (CGS-M). **Author contributions:** The overall experimental design was conceived by P.D.M., J.S.H., and J.W.S., and together, they coordinated the full project. P.D.M., Z.C.T., and D.T.B. designed the PEP and GRIP experiments and carried out data collection and analysis. J.S.H. and H.E.W. designed the GaMA experiment and carried out data collection and analysis. J.W.S., A.W.S., and K.R.W. designed the PIC and adaptation experiments and carried out data collection and analysis. P.D.M., Z.C.T., and D.T.B. developed the approaches for the multimodal feedback and bidirectional control prostheses. All authors also discussed and interpreted the experimental data and results. P.D.M., J.S.H., and J.W.S. wrote and edited the paper with writing contributions from all coauthors. **Competing interests:** The authors declare that they have no competing interests. **Data and materials availability:** All data needed to evaluate the conclusions in the paper are present in the paper or the Supplementary Materials.

Submitted 19 October 2020
Accepted 5 August 2021
Published 1 September 2021
10.1126/scirobotics.abf3368

Citation: P. D. Marasco, J. S. Hebert, J. W. Sensinger, D. T. Beckler, Z. C. Thumser, A. W. Shehata, H. E. Williams, K. R. Wilson, Neurorobotic fusion of prosthetic touch, kinesthesia, and movement in bionic upper limbs promotes intrinsic brain behaviors. *Sci. Robot.* **6**, eabf3368 (2021).

Science Robotics

Neurorobotic fusion of prosthetic touch, kinesthesia, and movement in bionic upper limbs promotes intrinsic brain behaviors

Paul D. Marasco, Jacqueline S. Hebert, Jonathon W. Sensinger, Dylan T. Beckler, Zachary C. Thumser, Ahmed W. Shehata, Heather E. Williams, and Kathleen R. Wilson

Sci. Robot. **6** (58), eabf3368. DOI: 10.1126/scirobotics.abf3368

Science Robotics (ISSN 2470-9476) is published by the American Association for the Advancement of Science. 1200 New York Avenue NW, Washington, DC 20005. The title *Science Robotics* is a registered trademark of AAAS.